Available online at www.sciencedirect.com
SCIENCE DIRECT®
Journal of Power Sources 124 (2003) 163–169
JOURNAL OF POWER SOURCES
www.elsevier.com/locate/jpowsour

Characterization and preparation of NiO-V_2O_5 composite film cathodes

Hai-Rong Liu, Yan-Qiu Chu, Zheng-Wen Fu, Qi-Zong Qin*

Chemistry Department, Laser Chemistry Institute, Fudan University, 220 Handan Road, Shanghai 200433, China

Received 16 January 2003; received in revised form 21 April 2003; accepted 12 May 2003

Abstract

NiO-V_2O_5 composite films have been fabricated by 355 nm pulsed laser reactive deposition using mixed metallic Ni and V targets with different molar ratios. The optimal deposition conditions of NiO-V_2O_5 composite films are found to be the substrate temperature of 300 °C and 100 mTorr O_2 ambient. X-ray diffraction (XRD) and scanning electron microscopy (SEM) analyses showed that the crystallinity of the NiO-V_2O_5 composite films gradually decreased with increasing the amount of nickel oxide and transformed to amorphous phase as the molar ratio of NiO/V_2O_5 (x) approaches 0.5. The amorphous $(NiO)_{0.5}V_2O_5$ composite film electrode exhibited a specific capacity of 340 mAh/g at a discharge rate of 2 C upon cycling with no obvious fading up to 500 cycles. XRD and X-ray photo-electron spectroscopy (XPS) measurements of NiO-V_2O_5 composite film electrodes revealed that there exists two electrochemical processes upon cycling. During the first discharge, the Li ions insertion process is accompanied by the reduction of NiO into metallic Ni. Then, the reversible processes involving Li ions insertion/extraction in V_2O_5 matrix and oxidation/reduction of Ni and Li_2O take place upon the subsequent cycling.

Keywords: Li-ion batteries; Cathode material; Thin film; Nickel oxide-vanadium oxide composite film; Pulsed laser deposition

1. Introduction

Transitional metal oxides and sulfides have been extensively investigated in the past decades for their use as electrode materials in rechargeable lithium-ion batteries [1–3]. Among them, vanadium pentoxide is one of the most promising cathode materials because it can exhibit high insertion level of Li^+ ions, resulting in a high specific energy density. However, V_2O_5 has a drawback in that its crystal structure can be easily destroyed upon discharge and charge cycling, thereby leading to capacity fade. The poor capacity retention of V_2O_5 electrode upon cycling limits its use in practical batteries. Many efforts have been made to improve the cycle life of the V_2O_5 electrode. It is well known that the structure and morphology of V_2O_5 can strongly influence its electrochemical performance [4]. Several different structure of V_2O_5 electrodes have been developed, which exhibited improved electrochemical properties. For instance, the high surface area V_2O_5 aerogel electrode exhibits a larger lithium intercalation capacity [5]. Moreover, the nano-structured V_2O_5 fabricated by template method can retain the charge and discharge cycleability even at a high discharge rate [6].

Recently, a variety of V_2O_5-based composite electrodes such as M^{2+}-V_2O_5 (M: Ni, Mn, Co, Cu, Ag) [7–9] and MO-V_2O_5 (M: Ni, Ti) [10,11] have received considerable attentions. For instance, the electrochemical insertion processes of lithium ions into Ni-V_2O_5 (Ni/V = 0.075) have been investigated by Inagaki et al. [7]. They found that charge balance and lattice site were two important factors which governed the foreign ions, such as Li^+ and Ni^{2+}, inserting into V_2O_5 lattice. Recently, Lourenco et al. fabricated vanadium–nickel mixed oxides thin films as promising electrode materials by rf sputtering [10], these electrode materials exhibited large capacity and good electrochemical reversibility upon cycling for several hundreds cycles at a current density of 50 μA/cm^2. Although previous studies have been done, it is necessary to do more works for further exploration of the electrochemical reaction mechanism of NiO-V_2O_5 composite film electrodes and improvement of their specific capacity and cycleability.

In our laboratory, thin film electrodes such as Ta_2O_5 [12], NiO [13] and Ag-V_2O_5 composite films [14] have been successfully prepared by pulsed laser reactive deposition method and exhibited excellent electrochemical properties. In this work, the NiO-V_2O_5 composite films were fabricated by pulsed laser deposition (PLD) method starting from mixed metallic Ni and V targets with different

* Corresponding author. Fax: +86-21-6510-2777.
E-mail address: qzqin@fudan.ac.cn (Q.-Z. Qin).

0378-7753/$ – see front matter © 2003 Elsevier B.V. All rights reserved.
doi:10.1016/S0378-7753(03)00597-4

molar ratio. X-ray diffraction (XRD), scanning electron microscopy (SEM), X-ray photo-electron spectroscopy (XPS) and electrochemical measurements were performed to investigate the influence of NiO molar amount in $(NiO)_xV_2O_5$ on the structure. The electrochemical reaction mechanism of $(NiO)_xV_2O_5$ composite film electrode with lithium during the discharge and charge cycle is also discussed.

2. Experimental

The NiO-V_2O_5 composite films were fabricated by PLD method. The experimental set up used for PLD has been described elsewhere [15]. A 355 nm laser beam provided by the third harmonic frequency of a Q-switch Nd:YAG laser (Spectra Physics GCR-150) was focused on the rotatable target with an angle of 45° to the surface normal. The repetition rate was 10 Hz with a pulse width of 6 ns, and the laser fluence was about 2 J/cm^2. The deposition chamber was evacuated to a base pressure of about 0.01 mTorr, and then pure O_2 gas (99.9%) was introduced into the chamber and remained at a pressure of 100 mTorr. The films were deposited on stainless steel substrates. The target–substrate distance was 3 cm. The targets were prepared by mixing the stoichiometric amount of nickel powder (99.5%) with vanadium powder (99.5%) in a molar ratio Ni/2V (x) ranging from 0.1 to 0.5, and then pressed to form 1.3 cm diameter pellets. The deposition time was kept 1 h and the thin film weight on the substrate could be calculated to be 6.6×10^{-5} g from the density (3.3 g/cm^3), the thickness (200 nm) and the surface area of as-deposited film (1 cm^2). The thickness was determined by SEM and confirmed by a surface profilometer (Tencor Alpha Step 200).

For the electrochemical measurements, a simple three-electrode system was employed, in which the deposited films served as the working electrode, and two metallic lithium sheets were used as both reference and counter electrodes. The electrolyte consisted of 1 M $LiPF_6$ ethylene carbonate (EC)/dimethyl carbonate (DMC) with ratio of 1/1 (w/w) (Merck). The cells were assembled in a glove box filled with argon. The chronopotentiometric data were acquired using LAND cell-testing system.

Film crystallinity and morphology were characterized by X-ray diffraction with a Rigata/max-C diffractometer with Cu Kα radiation and scanning electron microscopy (Philips XL 30), respectively. X-ray photo-electron spectroscopy measurements were performed on a Perkin-Elmer PHI 5000C ESCA system with monochromatic Al Kα

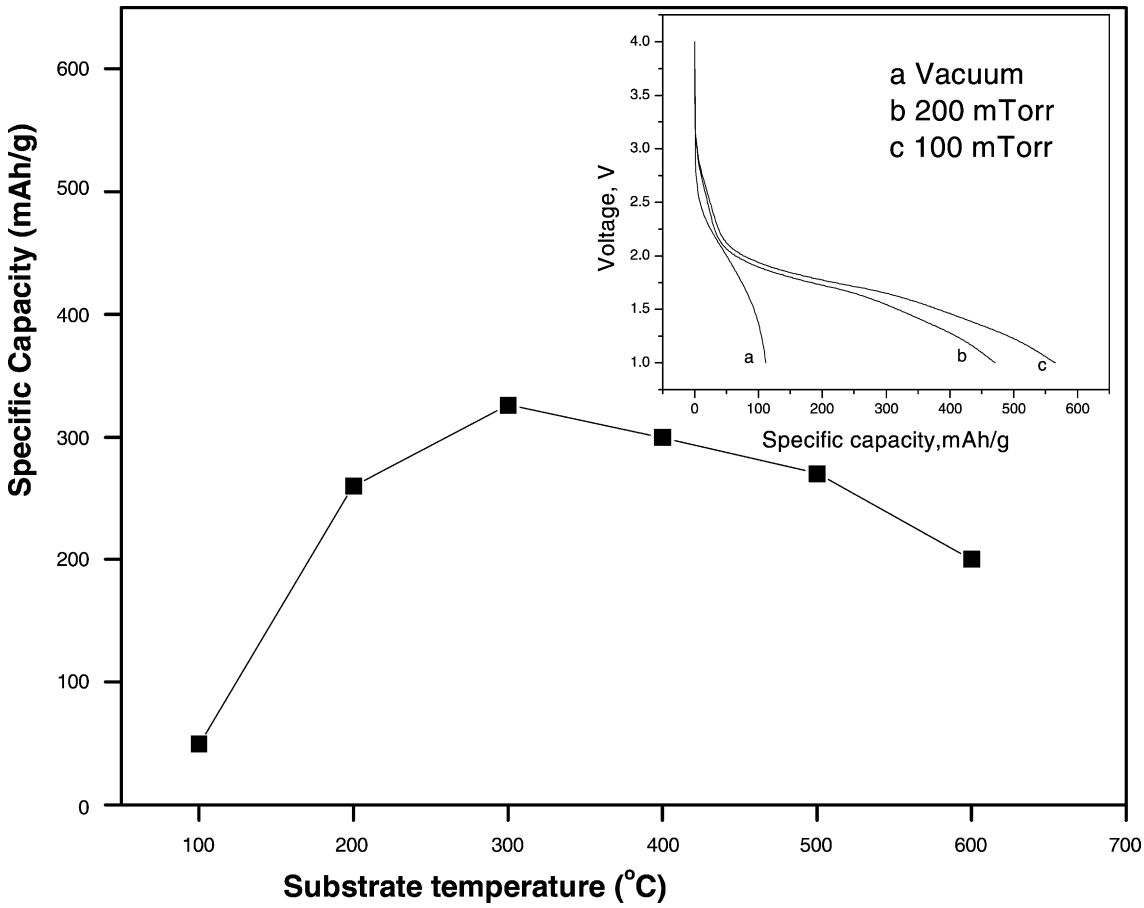

Fig. 1. The discharge capacity of the $(NiO)_{0.5}V_2O_5$ composite film electrode as a function of the substrate temperature. The inset shows the initial discharge curves of $(NiO)_{0.5}V_2O_5$ composite films deposited at different pressure of ambient oxygen pressure.

(1486.6 eV) irradiation. Pulsed laser deposition method is generally considered to be effective in fabricating thin films with the stoichiometry of the targets. The chemical composition of the as-deposited $(NiO)_xV_2O_5$ composite film was determined by energy-dispersive X-ray analysis (EDX) and inductive coupled plasma (ICP) emission spectrometer. Our results indicated that the molar ratio Ni/V of the film is close to the nominal composition of target.

3. Results and discussion

Previous studies [16] have showed that the crystallinity and morphology as well as electrochemical performance of V_2O_5 film prepared by pulsed laser reactive ablation depended strongly on film growth conditions such as the substrate temperature and ambient gas pressure. Fig. 1 presents the relationship between the discharge capacity of $(NiO)_{0.5}V_2O_5$ composite film and substrate temperature (°C) in a 100 mTorr O_2 ambient. It can be seen that the discharge capacity of film electrode at a rate of 2 C increases with increase in the substrate temperature and reaches the maximum value at $T_s = 300$ °C. Then, the discharge capacity drops with increase in the substrate temperature. The inset in Fig. 1 shows the initial discharge curves of $(NiO)_{0.5}V_2O_5$ composite films deposited at different pressure of ambient oxygen pressure. The discharge capacity

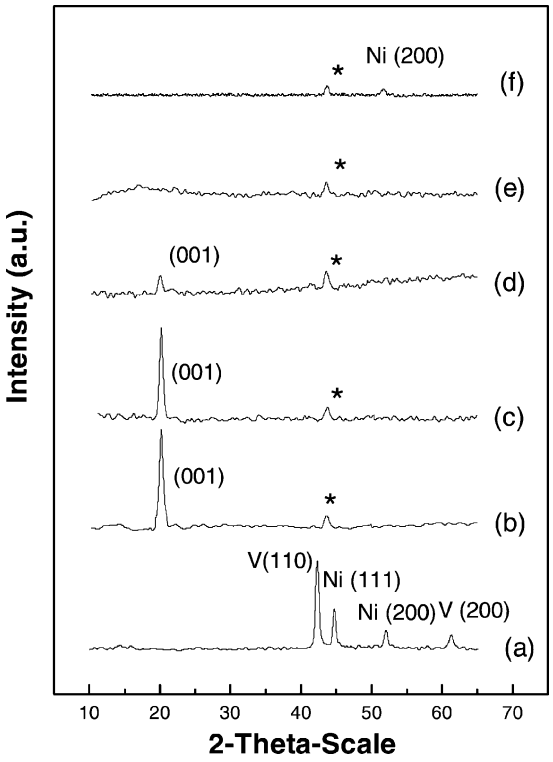

Fig. 2. X-ray diffraction patterns: (a) mixed metallic Ni–V target; (b) V_2O_5 film; (c) $(NiO)_{0.1}V_2O_5$ film; (d) $(NiO)_{0.3}V_2O_5$ film; (e) $(NiO)_{0.5}V_2O_5$ film; (f) lithiated $(NiO)_{0.5}V_2O_5$ film at 1.0 V. The peaks marked with an asterisk correspond to stainless steel substrate.

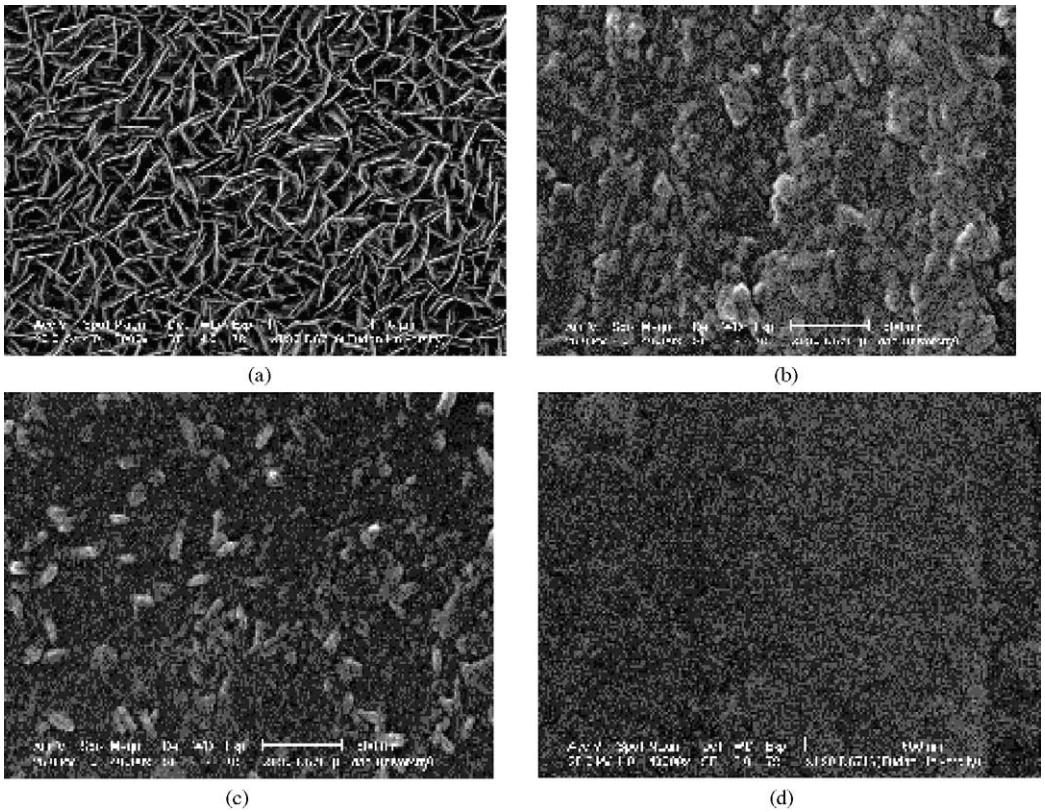

Fig. 3. SEM images of as-deposited films: (a) V_2O_5; (b) $(NiO)_{0.1}V_2O_5$; (c) $(NiO)_{0.3}V_2O_5$; (d) $(NiO)_{0.5}V_2O_5$.

of $(NiO)_{0.5}V_2O_5$ composite film deposited at vacuum was considerably low, which may result from deficiency of oxygen during pulsed laser deposition process. However, the discharge capacity of composite film deposited at 200 mTorr was slightly lower than that of $(NiO)_{0.5}V_2O_5$ composite film deposited at 100 mTorr. Accordingly, the optimal conditions for depositing the $(NiO)_{0.5}V_2O_5$ composite films are $T_s = 300\,^{\circ}C$ in 100 mTorr O_2 ambient.

Fig. 2 presents the XRD patterns mixed metallic target and as-deposited NiO-V_2O_5 composite films with different molar ratio (x) of NiO/V_2O_5. The XRD pattern of mixed metallic target exhibits four diffraction peaks, which can be identified as (1 1 0), (2 0 0) reflections of metallic V and (1 1 1), (2 0 0) reflections of metallic Ni, respectively. For the deposited films, all of these peaks disappear. This result indicates that metallic Ni and V has completely reacted with oxygen gas and converted to metal oxide composite films after pulsed laser deposition. Apart from the diffraction peak of the stainless steel substrate, a new peak appears at $2\theta = 20.2$, which can be assigned to (0 0 1) reflection of orthorhombic structure of V_2O_5. The intensity of (0 0 1) peak decreases gradually from NiO-V_2O_5 composite film with $x = 0.1$–0.5, and this peak disappears completely for $(NiO)_{0.5}V_2O_5$ film. It indicates that the layered structure of orthorhombic V_2O_5 film changes into an amorphous phase with increasing the NiO amount in the composite films. It should be noted that a new peak appeared at $2\theta = 20.24$ for the $(NiO)_{0.5}V_2O_5$ composite film discharged at 1.00 V, which can be attributed to the (2 0 0) reflection peak of metallic nickel. This result implies that the NiO in $(NiO)_{0.5}V_2O_5$ composite film can be reduced to metallic nickel when the composite film is lithiated to 1.00 V.

The surface morphologies for the pure V_2O_5 and NiO-V_2O_5 composite films exhibit distinct difference as shown in Fig. 3. It can be seen that the pure V_2O_5 film deposited on stainless steel substrate is composed of a high density of dendrite grains (0.1–0.2 μm width and 1 μm length). However, the grain shape of the NiO-V_2O_5 composite film changes obviously comparing with pure V_2O_5 film and is dependent on the NiO amount (x) in the composite films. The grain size seems to decrease with the increase in NiO amount (x) in the composite films, and rarely grains were observed on the surface for $(NiO)_{0.5}V_2O_5$ composite films. Combined with our XRD results, it is reasonable to suggest that the polycrystalline structure of V_2O_5 can be destroyed and gradually transformed to amorphous phase as a result of the insertion of nickel oxide into V_2O_5 during the pulsed laser deposition.

The V 2p and Ni 2p core levels XPS spectra of as-deposited NiO-V_2O_5 composite films were examined as shown in Fig. 4. The peak position of V $2p_{3/2}$ and $2p_{1/2}$ are observed at 516.4 and 523.8 eV, which agrees with the reported values for V_2O_5 [17]. No obvious chemical shifts of vanadium are found in the composite films, implying that the chemical state of vanadium was V^{5+} in the composite films. This result is in agreement with the XRD results described above. It should be noted that Ni $2p_{3/2}$ and $2p_{1/2}$ peaks for $(NiO)_{0.1}V_2O_5$ and $(NiO)_{0.5}V_2O_5$

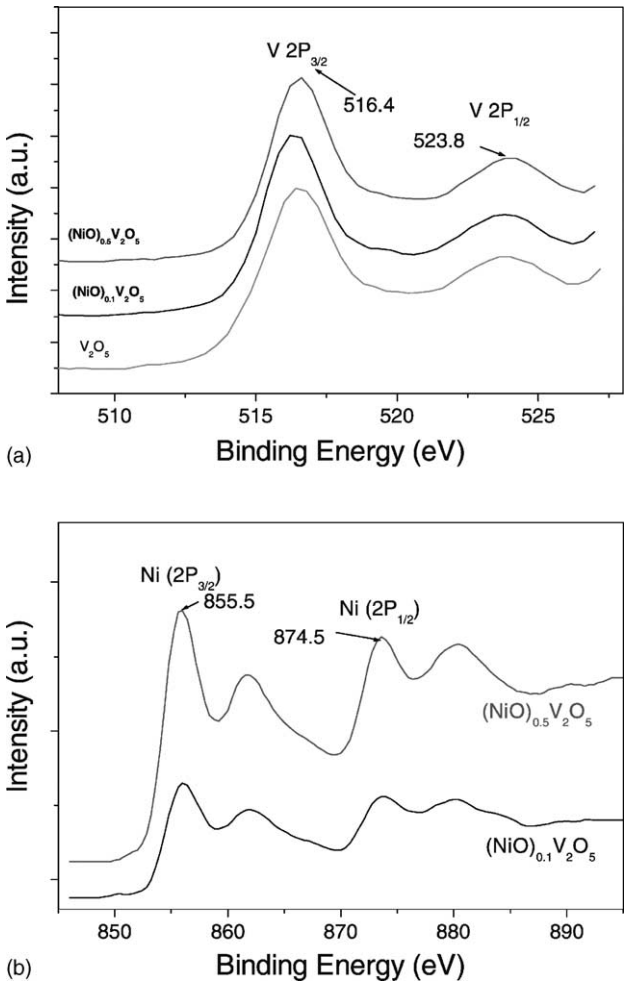

Fig. 4. XPS spectra of as-deposited V_2O_5, $(NiO)_{0.1}V_2O_5$ and $(NiO)_{0.5}V_2O_5$ composite films: (a) V 2p; (b) Ni 2p.

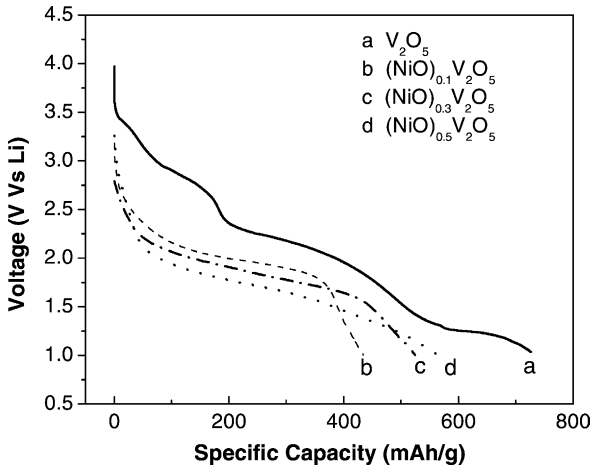

Fig. 5. The initial discharge behavior of V_2O_5 film and $(NiO)_xV_2O_5$ composite film electrodes at 0.5 C rate.

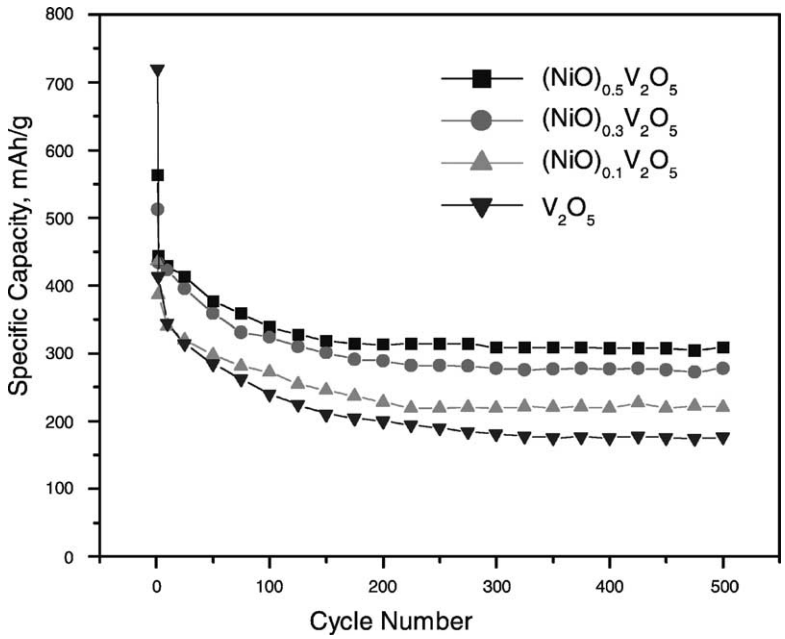

Fig. 6. Discharge capacities vs. cycle number for V_2O_5 film and $(NiO)_xV_2O_5$ composite film electrodes at 0.5 C rate.

composite films have the same peak position and appear at 855.5 and 874.5 eV, respectively. According to the reported values [18], these peaks correspond to the valence state of Ni^{2+} in NiO. These evidences also indicate that the composite films are composed of V_2O_5 and NiO.

As we know, the different initial discharge curve can provide much information of the different phase of the film electrode. Fig. 5 presents the measured initial discharge curves of pure V_2O_5 and NiO-V_2O_5 composite film electrodes with different molar ratio (x). It can be seen that the pure V_2O_5 film electrode has a stepwise discharge curve, indicating a polycrystalline film. However, the discharge curves gradually become more monotonic with increasing of nickel oxide amount in $(NiO)_xV_2O_5$ composite film electrodes and the plateau disappears completely in $(NiO)_{0.5}V_2O_5$ composite film electrodes, indicating a typical electrochemical behavior of amorphous film electrode. The phase and structure change of $(NiO)_xV_2O_5$ composite film electrode obtained from their initial discharge measurements is in agreement with the results obtained from XRD and SEM mentioned above.

Fig. 6 shows that $(NiO)_xV_2O_5$ composite electrodes with $x = 0.1, 0.3, 0.5$ have the higher capacities than the

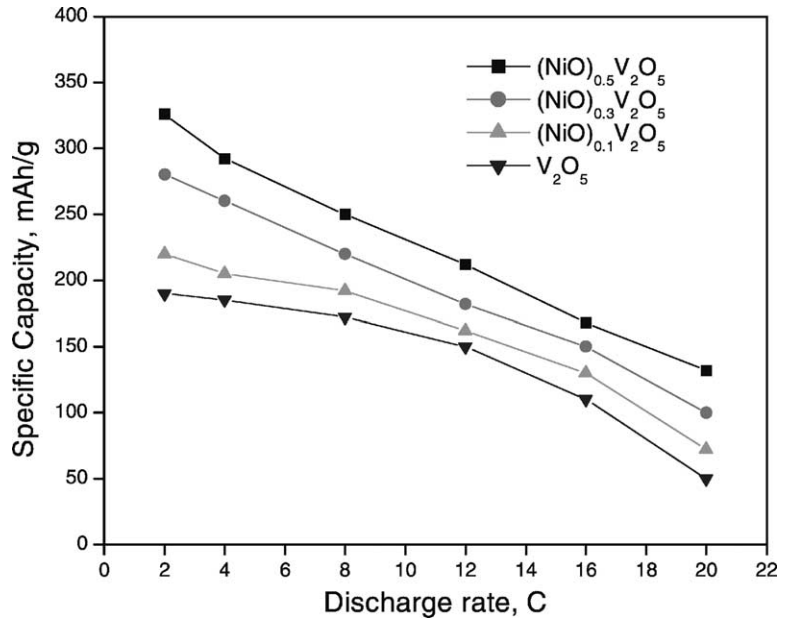

Fig. 7. The rate performance for V_2O_5 and $(NiO)_xV_2O_5$ film electrodes cycled between 3.8 and 1.0 V at different discharge rate.

pure V_2O_5 film electrode when cycling at a same rate of 2 C. It should be noted that the amorphous $(NiO)_{0.5}V_2O_5$ composite film electrode has the highest specific capacity comparing to the others and this composite film electrodes still retained a capacity of 340 mAh/g with no obvious fading upon cycling for over more than 500 cycles. The discharge capacity of $(NiO)_{0.7}V_2O_5$ was estimated to be 300 mAh/g. Comparing with $(NiO)_{0.5}V_2O_5$, the capacity of $(NiO)_{0.7}V_2O_5$ is lower. But the reason is rather complicated.

The discharge capacities of pure V_2O_5 and $(NiO)_xV_2O_5$ film electrodes at different discharge rate are presented in Fig. 7. It can be seen that the discharge capacity decreases with increasing of the discharge rate when these electrodes are cycled between 3.8 and 1.0 V. However, the $(NiO)_xV_2O_5$ film electrodes exhibit higher rate performance than pure V_2O_5 film electrode. A discharge capacity of 132 mAh/g was obtained for the $(NiO)_{0.5}V_2O_5$ film electrode at discharge rate as high as 20 C.

The electrochemical reaction mechanisms of NiO-V_2O_5 composite film electrodes with lithium ion were investigated by ex situ XPS measurements. The ex situ XPS spectra of V 2p and Ni 2p for the $(NiO)_{0.5}V_2O_5$ composite film electrodes after the first discharge are shown in Fig. 8. It can be seen that the XPS spectra of lithiated film are different from those of as-deposited film. The measured V $2p_{3/2}$ and V $2p_{1/2}$ peaks shift toward higher energy positions and appear at 518.0 and 524.0 eV, respectively. Such a shift is considered due to the effect of carbon oxide or hydroxide on the film surface contamination. However, the binding energy of Ni $2p_{3/2}$ peak is found to shift from 855.5 eV toward lower energy and appears at 852.4 eV, which can be assigned to the binding energy of metallic Ni [18]. It implies that NiO in the lithiated $(NiO)_{0.5}V_2O_5$ composite film is reduced to metallic Ni when lithium ions inserted into the composite film electrode. The Li 1s XPS spectrum for the lithiated composite film is presented in the inset, in which the binding energy of 55.9 eV could be attributed to that of Li_2O (55.6 eV), indicating the formation of Li_2O [19].

Based on the XPS and XRD results for as-deposited and lithiated $(NiO)_{0.5}V_2O_5$ composite film electrodes, two kinds of lithiated processes are proposed for the $(NiO)_{0.5}V_2O_5$ composite film. When the Li ions react with the composite film electrode, a part of Li ions inserts and releases from the vacant position within the layered structure of V_2O_5 in composite film. Meanwhile, the other part of Li ions react with NiO in composite film and the NiO can be reduced, leading to the formation of metallic Ni and Li_2O. The insertion and extraction of Li ions in the V_2O_5 matrix accompanied with the reduction/oxidation of nickel oxide in the NiO-V_2O_5 composite film electrodes can be expressed as:

$$(x + 2y)\mathrm{Li} + (\mathrm{NiO})_yV_2O_5 \leftrightarrows \mathrm{Li}_xV_2O_5 + y\mathrm{Ni} + y\mathrm{Li}_2O.$$

Both of two processes contribute to the specific capacity of the (NiO)-V_2O_5 composite film electrode. In order to further confirm above mechanism, the XRD of delithiated NiO-V_2O_5 film electrodes were examined. However, we did not observe the (0 0 1) peak for V_2O_5, which may be due to an amorphous structure of V_2O_5 or the nano-sized delithiated V_2O_5 smaller than the X-ray coherence length. The amorphization of polycrystalline structure upon cycling was also observed in the other vanadium-based electrode materials [20].

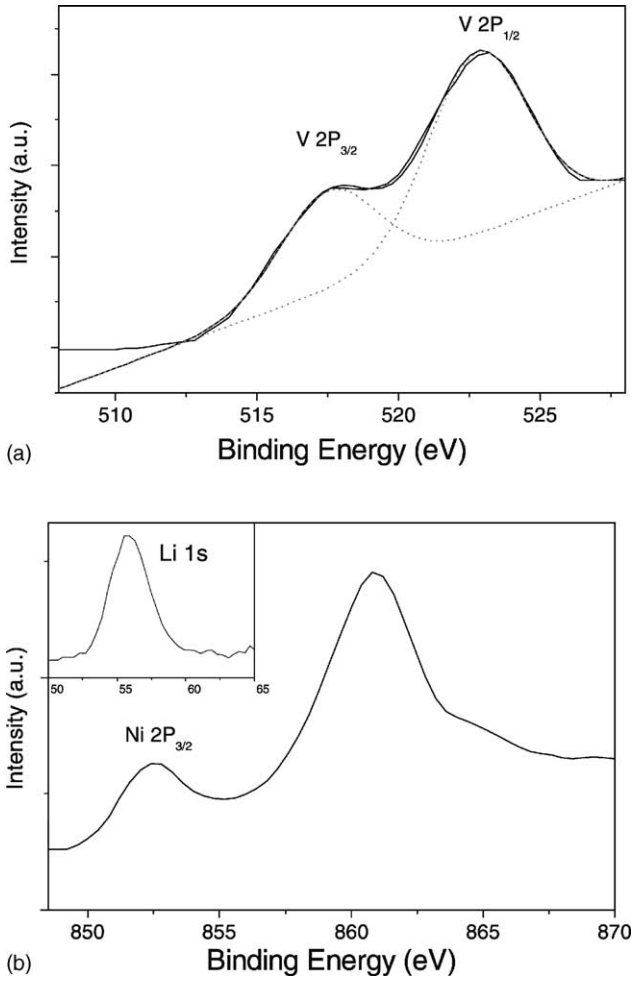

Fig. 8. XPS spectra of lithiated $(NiO)_{0.5}V_2O_5$ composite film electrode: (a) V 2p; (b) Ni 2p.

4. Conclusions

NiO-V_2O_5 composite films have been prepared by reactive pulsed laser deposition in 100 mTorr oxygen ambient at a substrate temperature of 300 °C. X-ray diffraction and scanning electron microscopy analyses showed that the crystallinity of the NiO-V_2O_5 composite films depended strongly on the amount of nickel oxide and transformed to amorphous phase as the molar ratio of NiO/V_2O_5 increases to 0.5. These NiO-V_2O_5 composite film electrodes demonstrated stable cycleability between 3.8 and 1.0 V versus Li at a discharge rate of 2 C upon cycling with no obvious fading

up to 500 cycles. The proposed electrochemical mechanisms of $(NiO)_{0.5}V_2O_5$ composite film electrode can be expressed by the following steps. During the first discharge of $(NiO)_{0.5}V_2O_5$ composite film electrode, the insertion of Li ions into V_2O_5 matrix is accompanied by the reduction of amorphous NiO into metallic Ni. Then the subsequent charge/discharge cycles are reversible, which including the Li ions insertion and extraction in the V_2O_5 matrix and the oxidation/reduction reactions of Ni and Li_2O. Both these processes contribute to the specific capacity of the (NiO)-V_2O_5 composite film electrodes.

Acknowledgements

This work was supported by the National Nature Science Foundation of China (Project nos. 200083001 and 20203006). The authors would like to thank Professor Qi-Ke Zheng for valuable discussions.

References

[1] S. Choi, A. Manthirum, J. Elecrochem. Soc. 149 (2002) A162.
[2] I.M. Kotschau, J.R. Dahn, J. Elecrochem. Soc. 145 (1998) 2672.
[3] S.D. Jones, J.R. Akridge, F.K. Shokoohi, Solid State Ionics 69 (1994) 357.
[4] J. Livage, Chem. Mater. 3 (1991) 578.
[5] S. Passerini, J.J. Ressler, D.B. Le, W.H. Smyrl, Electrochim. Acta 44 (1999) 2209.
[6] C.J. Patrissi, C.R. Martin, J. Elecrochem. Soc. 146 (1999) 3176.
[7] M. Inagaki, K. Omori, T. Tsumura, T. Watanabe, A. Shimizu, Solid State Ionics 78 (1995) 275.
[8] F. Coustier, J. Hill, B.B. Owens, S. Passerini, W.H. Smyrl, J. Power Sources 146 (1999) 1355.
[9] J.K. Takeuchi, A.C. Marschilok, S.M. Davis, R.A. Leising, E.S. Takeuchi, Coord. Chem. Rev. 219–221 (2001) 283.
[10] A. Lourenco, E. Masetti, F. Decker, Electrochim. Acta 46 (2001) 2257.
[11] C. Bellenger, C. Chermarin, D. Deroo, S. Maximovitch, A. Surca Vuk, B. Orel, Electrochem. Acta 46 (2001) 2263.
[12] Z.W. Fu, Q.Z. Qin, J. Elecrochem. Soc 147 (2000) 4610.
[13] Y. Wang, Q.Z. Qin, J. Elecrochem. Soc. 149 (2002) A873.
[14] Y.Q. Chu, Q.Z. Qin, Chem. Mater. 14 (2002) 3152.
[15] Z. W Fu, J.L. Kong, Q.Z. Qin, J. Electrochem. Soc. 146 (1999) 3914.
[16] J. Zhang, J.M. McGraw, J. Turner, P. Ginley, J. Electrochem. Soc. 144 (1997) 1630.
[17] Y. Hattori, T. Konishi, K. Kaneko, Chem. Phys. Lett. 355 (2002) 37.
[18] M. Schulze, R. Reissner, M. Lorenz, U. Radke, W. Schnurnberger, Electrochim. Acta 44 (1999) 3969.
[19] J.F. Moulder, W.F. Stickle, P.E. Sobol, K.O. Bomben, Handbook of X-ray Photoelectron Spectroscopy, Physical Electronics Division, Eden Prairie, 1992.
[20] S.S. Kim, H. Ikuta, Solid State Ionics 139 (2001) 57.